Self–Consistent Conserving Theory for Quantum Impurity Systems: Renormalization Group Analysis*

Stefan Kirchner and Johann Kroha

Institut für Theorie der Kondensierten Materie, Universität Karlsruhe
Postfach 6980, 76128 Karlsruhe, Germany

We review the diagrammatic, conserving theory for quantum impurities with strong on-site repulsion. The method is based on auxiliary particle technique, where Wick's theorem is valid, which opens up the possibility for generalizations to more complicated situations. An analysis in terms of the perturbative renormalization group (RG) shows that on the level of the Conserving T–matrix Approximation the theory correctly describes the RG flow, including the non-scaling of potential scattering terms and the correct Kondo temperature.

PACS numbers: 71.27.+a, 71.10.Fd, 75.20.Hr, 11.10.Hi.

1. INTRODUCTION

The physics of correlated electron systems on a lattice, such as heavy fermion compounds or narrow band metals is determined by a strong on–site repulsion between the electrons. It can lead to the formation of local magnetic moments and, subsequently, either to the Kondo effect[1] or to magnetic ordering, to a Mott–Hubbard metal–insulator transition, and even to superconductivity. The theoretical description of such systems has been greatly advanced by the dynamical mean field theory (DMFT),[2,3] where the lattice system is mapped onto an effective single–impurity Anderson model, embedded self–consistently in a correlated electron bath. Thus, the complexity of the lattice system is reduced to that of a quantum impurity problem. Quantum impurity systems are also of central interest in their own right: The Anderson impurity model is the standard model, e.g.,

*Dedicated to Peter Wölfle on the occasion of his 60th birthday.

for the description of quantum dots in the Coulomb blockade and Kondo regimes[4,5,6], of scanning tunneling spectroscopy (STS) on magnetic ions on a metal surface[7,8,9], and for the investigation of single–impurity physics in heavy fermion systems[10,11]. Therefore, it is highly desirable to construct theoretical methods flexible enough to describe quantum impurities with a complex structure of the fermionic bath (in DMFT), with multiple local orbitals (in rare earth systems, quantum dots etc.), and which can readily be generalized to non–equilibrium transport. Existing exact solution methods like Bethe ansatz, conformal field theory (CFT), and numerical renormalization group (NRG) are lacking this flexibility to a large extent.

A general method, based on the auxilary particle technique[12] (where Wick's theorem is valid), which is capable of describing quantum impurity systems over the complete temperature range from the weak to the strong coupling regime and which, as a diagrammatic method, offers the above–mentioned flexibility, has been envisaged by Peter Wölfle starting in the late 1980s, even before the advent of DMFT and before the technological break–through that made the fabrication of Kondo quantum dots[13,14,15] possible. Such a method, now termed *Conserving T–Matrix Approximation* (CTMA), has subsequently been developed[16,17,18,19], and has been shown to describe, as an example of physical quantities, the spin susceptibility of the single– and the two–channel Anderson impurity model correctly from the high temperature regime down to the lowest temperatures T considered of about $1/100$ of the Kondo scale T_K [20,21].

The choice of diagrams comprising the CTMA has been justified in terms of principal diagrams[17,21], where in each order of the impurity hybridization the dominant term in the spin as well as in the charge fluctuation channel are taken into account. In the present paper we present another check for the validity of the CTMA: The renormalization group flow of the coupling constants appearing in the spin and charge vertices defined by the CTMA should be the same as the *exact* flow of the respective coupling constants of the Anderson impurity model at least in the weak coupling regime. By self–consistency, the CTMA may then be expected to reach the correct strong coupling behavior. We note that this scheme might be extended to be used as a guiding principle for the construction of approximative strong coupling methods for other models like the Hubbard and t-J–models[23].

The paper is organized as follows. After a brief overview of the auxiliary particle technique and its exact properties in Section 2, the conserving approximations for the Anderson impurity model, the *Non–Crossing Approximation* (NCA) and the *Conserving T–Matrix Approximation* (CTMA), will be defined in Section 3. Section 4 contains the perturbative renormalization group analysis of both the NCA and the CTMA in the sense discussed

above. Some conlusions are drawn in Section 5.

2. EXACT PROPERTIES OF THE AUXILIARY PARTICLE TECHNIQUE

The large on–site repulsion U between electrons in the local d–orbital of an Anderson impurity effectively restricts the dynamics to the sector of Fock space with no double occupancy. It can be implemented using the auxiliary or slave boson method[12], where in the limit $U \to \infty$ the creation operator for an electron with spin σ in the d-level is written in terms of the auxiliary fermion operators f_σ and boson operators b as $d_\sigma^\dagger = f_\sigma^\dagger b$. This representation is exact, if the constraint on the total auxiliary particle number operator, $\hat{Q} = \sum_\sigma f_\sigma^\dagger f_\sigma + b^\dagger b \equiv 1$, is fulfilled. $f_\sigma^\dagger$ and $b^\dagger$ may be envisaged as creating the three allowed states of the impurity: singly occupied with spin σ or empty. The Hamiltonian of a single Anderson impurity with local level E_d, embedded in a sea of conduction electrons (creation operators $c_{\vec{k}\sigma}^\dagger$, dispersion $\varepsilon_{\vec{k}}$, half band width D, and density of states at the Fermi level N_0) via a hybridization matrix element V then reads ($U \to \infty$),

$$H = \sum_{\vec{k},\sigma} \varepsilon_{\vec{k}} c_{\vec{k}\sigma}^\dagger c_{\vec{k}\sigma} + E_d \sum_\sigma f_\sigma^\dagger f_\sigma + V \sum_{\vec{k},\sigma} (c_{\vec{k}\sigma}^\dagger b^\dagger f_\sigma + h.c.) \ . \tag{1}$$

In the Kondo regime, $N_0 J_0 \equiv N_0 V^2/|E_d| \ll 1$, the model has a low temperature scale, the Kondo temperature $T_K \simeq D\mathrm{e}^{-1/(2N_0 J_0)}$, at which the system crosses over from singular spin scattering to a spin–screened, strong coupling Fermi liquid (FL) ground state.[1]

2.1. Exact Projection onto the Physical Fock Space

The auxiliary particle Hamiltonian (1) is invariant under simultaneous, local $U(1)$ gauge transformations, $f_\sigma \to f_\sigma \mathrm{e}^{i\phi(\tau)}$, $b \to b\mathrm{e}^{i\phi(\tau)}$, with $\phi(\tau)$ an arbitrary, time dependent phase. While the gauge symmetry guarantees the conservation of the local, integer charge Q, it does not single out any particular Q sector, like $Q = 1$. In order to project onto the $Q = 1$ sector of Fock space, one may use the following procedure[24,25]: Consider first the grand-canonical ensemble with respect to Q and the associated chemical potential $-\lambda$. The expectation value in the $Q = 1$ subspace of any physical operator $\hat{A}$ acting on the impurity states is then obtained exactly as

$$\langle \hat{A} \rangle = \lim_{\lambda\to\infty} \frac{\frac{\partial}{\partial\zeta}\mathrm{tr}[\hat{A}e^{-\beta(H+\lambda Q)}]_G}{\frac{\partial}{\partial\zeta}\mathrm{tr}[e^{-\beta(H+\lambda Q)}]_G} = \lim_{\lambda\to\infty} \frac{\langle \hat{A} \rangle_G}{\langle Q \rangle_G} \ , \tag{2}$$

where the index G denotes the grand canonical ensemble, ζ denotes the fugacity $\zeta = \mathrm{e}^{-\beta\lambda}$, and $-\lambda$ is by construction the chemical potential associated with the local charge Q. In the second equality of Eq. (2) we have used the fact that any physical operator $\hat{A}$ acting on the impurity states is composed of the impurity electron operators d_σ, $d_\sigma^\dagger$, and thus annihilates the states in the $Q = 0$ sector, $\hat{A}|Q = 0\rangle = 0$. It is obvious that the grand-canonical expectation values involved in Eq. (2) may be factorized into auxiliary particle propagators using Wick's theorem, thus allowing for the application of standard diagrammatic techniques. For a detailed review see Ref. 21,22.

It is important to note that, in general, λ plays the role of a time dependent gauge field. In Eq. (2) a time independent gauge for λ has been chosen. In this way, the projection is only performed at one instant of time, explicitly exploiting the conservation of the local charge Q. This means that in the subsequent development of the theory, the Q conservation must be implemented exactly. It is achieved in a systematic way by means of conserving approximations[26], i.e. by deriving all self-energies and vertices by functional derivation from one common Luttinger-Ward functional Φ of the fully renormalized Green's functions,

$$\Sigma_{b,f,c} = \delta\Phi\{G_b, G_f, G_c\}/\delta G_{b,f,c}. \tag{3}$$

This amounts to calculating all quantities of the theory in a self-consistent way, but has the great advantage that gauge field fluctuations need not be considered.

2.2. Infrared Threshold Behavior of Auxilary Propagators

As seen from Eq. (2), the limit $\lambda \to \infty$ effecting the projection onto the physical subspace implies that the traces involved in the time ordered pseudofermion and slave boson Green's functions G_f, G_b are extended purely over the $Q = 0$ sector of Fock space, and thus the backward-in-time contribution to the auxiliary particle propagators vanishes. Consequently, the auxiliary particle propagators are formally identical to the core hole propagators appearing in the well-known X-ray problem[27], and the long-time behavior of G_f (G_b) is determined by the orthogonality catastrophe[28] of the overlap of the Fermi sea without impurity ($Q = 0$) and the fully interacting conduction electron sea in the presence of a pseudofermion (slave boson) ($Q = 1$). It may be shown that the auxiliary particle spectral functions have threshold behavior with vanishing spectral weight at $T = 0$ for energies ω below a threshold E_o, and power law behavior above E_o, $A_{f,b}(\omega) \propto \Theta(\omega - E_o)\omega^{-\alpha_{f,b}}$.

In the present paper we will consider only the single-channel Anderson model with its spin screened FL ground state, leaving the impurity as a

pure potential scatterer. In this case, the exact threshold exponents may be deduced [29,17,21] from an analysis in terms of scattering phase shifts[30], using the Friedel sum rule. One obtains for spin degeneracy $N \geq 1$ and conduction channel degeneracy $M = 1$,

$$\alpha_f = \frac{2n_d - n_d^2}{N} \ , \qquad \alpha_b = 1 - \frac{n_d^2}{N} \qquad (N \geq 1, M = 1) \ . \tag{4}$$

These results have been confirmed by numerical renormalization group (NRG) calculations[31] and by use of the Bethe ansatz solution in connection with boundary CFT[32]. We note in passing that, on the contrary, in the non–Fermi liquid (NFL) case of the multi-channel Kondo model ($M \geq N \geq 2$) the threshold exponents have been deduced by a CFT solution[33] as

$$\alpha_f = \frac{M}{M+N} \ , \qquad \alpha_b = \frac{N}{M+N} \qquad (M \geq N \geq 2) \ . \tag{5}$$

Since the dependence of α_f, α_b on the impurity occupation number n_d shown above originates from pure potential scattering, it is characteristic for the FL case. The auxiliary particle threshold exponents are, therefore, indicators for FL or NFL behavior in quantum impurity models of the Anderson type.

3. CONSERVING APPROXIMATIONS

The task in constructing a self–consistent, conserving theory for a given system consists in finding the proper Luttinger–Ward functional that yields a correct description for the respective strongly correlated model. In this section we describe two approximation schemes for the Anderson impurity model, the NCA and the CTMA.

In Matsubara representation the auxiliary particle Green's functions $G_{f,b}$ read in terms of the self–energies $\Sigma_{f,b}$,

$$G_{f,b}(i\omega_n) = \left\{ [G^0_{f,b}(i\omega_n)]^{-1} - \Sigma_{f,b}(i\omega_n) \right\}^{-1} \ , \tag{6}$$

where

$$G^0_{f\sigma}(i\omega_n) = (i\omega_n - E_d - \lambda)^{-1} \ , \qquad G^0_b(i\omega_n) = (i\omega_n - \lambda)^{-1} \tag{7}$$

are the respective free propagators. Since, as a consequence of the projection procedure $\lambda \to \infty$, the energy eigenvalues of $H + \lambda Q$ scale to infinity $\propto \lambda Q$, it is useful to take a gauge $\lambda = \lambda_0 + \lambda'$ with $\lambda' \to \infty$, to shift the zero of the auxiliary particle frequency scale by λ', and to determine λ_0 such that for $T = 0$ the threshold of the auxiliary particle spectral functions lies at

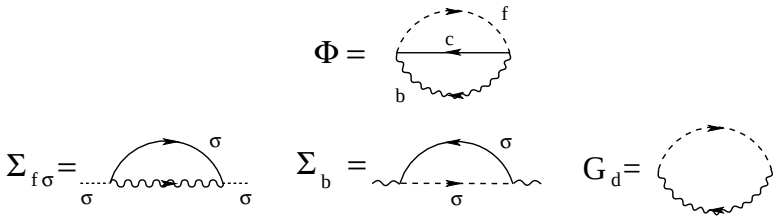

Fig. 1. Diagrammatic representation of the generating functional Φ of the NCA. Also shown are the pseudoparticle self–energies and the local d-electron Green's function derived from Φ, Eqs. (11)–(13). Throughout this article, dashed, wavy and solid lines represent fermion, boson, and conduction electron lines, respectively.

the frequency $\omega = 0$.[34] In particular, for vanishing hybridization the Green's functions read in this gauge,

$$G^0_{f\sigma}(i\omega_n) = (i\omega_n)^{-1} \ , \qquad G^0_b(i\omega_n) = (i\omega_n + E_d)^{-1} \ . \tag{8}$$

3.1. Non–Crossing Approximation (NCA)

The NCA as the simplest conserving approximation for the Anderson impurity model is motivated as a self–consistent expansion in terms of the hybridization parameter V which is assumed to be small. The NCA generating functional Φ is shown in Fig. 1. Also shown are the self–energies $\Sigma_{f,b}$ and the physical Green's function for an electron in the local d-level, G_d, generated from this by functional differentiation. They obey after analytic continuation to real frequencies ($i\omega \to \omega - i0$) and projection onto the physical subspace the following equations of self–consistent second order perturbation theory

$$\Sigma^{(NCA)}_{f\sigma}(\omega - i0) = \Gamma \int \frac{d\varepsilon}{\pi} f(\varepsilon) A^0_{c\sigma}(-\varepsilon) G_b(\omega + \varepsilon - i0) \tag{9}$$

$$\Sigma^{(NCA)}_{b}(\omega - i0) = \Gamma \sum_\sigma \int \frac{d\varepsilon}{\pi} f(\varepsilon) A^0_{c\sigma}(\varepsilon) G_{f\sigma}(\omega + \varepsilon - i0) \tag{10}$$

$$G^{(NCA)}_{d\sigma}(\omega - i0) = \int d\varepsilon \, \mathrm{e}^{-\beta\varepsilon} [G_{f\sigma}(\omega + \varepsilon - i0) A_b(\varepsilon) - A_{f\sigma}(\varepsilon) G_b(\varepsilon - \omega + i0)] \ , \tag{11}$$

where $\Gamma = \pi N_0 V^2$, and $A^0_{c\sigma} = \frac{1}{\pi} \mathrm{Im} G^0_{c\sigma}/N_0$ is the (unrenormalized) conduction electron density of states per spin, normalized to the density of states at the Fermi level N_0, $A_{f,b}(\omega) = \mathrm{Im} G_{f,b}(\omega - i0)$ denote the imaginary parts of the advanced propagators, and $f(\varepsilon) = 1/(\exp(\beta\varepsilon) + 1)$ is the

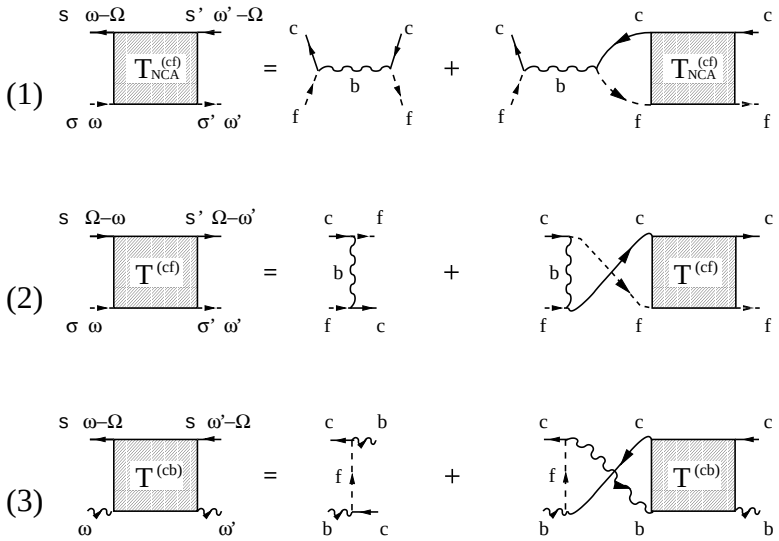

Fig. 2. Diagrammatic representation of the Bethe–Salpeter equation for (1) the conduction electron–pseudofermion p–h T-matrix $T^{(cf)}_{NCA}$, (2) the conduction electron–pseudofermion p–p T-matrix $T^{(cf)}$, Eq. (12), and (3) the conduction electron–slave boson T–matrix $T^{(cb)}$, Eq. (13). The external lines are drawn for clarity and do not belong to the T–matrices.

Fermi distribution function. Together with the expressions (6), (8) for the Green's functions, Eqs. (9)–(11) form a set of self–consistent equations for $\Sigma_{b,f,c}$, comprised of all diagrams without any crossing propagator lines[35,36]. For an efficient procedure for the numerical evaluation of the self–consistent equations at low T see Ref. 34. The solutions of the NCA equations have threshold power law behavior, with the exponents given by Eq. (5),[37] which are in disagreement with the correct exponents for the FL case, Eq. (4). As a consequence, the NCA does not correctly describe the FL regime of the Anderson impurity model, producing a spurious low energy singularity in the local d-electron spectrum, although it gives qualitatively correct results at high T and down to temperatures of about the Kondo scale T_K.

3.2. Conserving T-Matrix Approximation (CTMA)

In order to construct an aproximation which eliminates the shortcomings of the NCA mentioned above, the guiding principle has been to include those contributions to the vertex functions which capture the FL physics of the single–channel Anderson model below T_K, i.e. the formation of a collective singlet bound state of the local and of the conduction electron spins.[17,21]

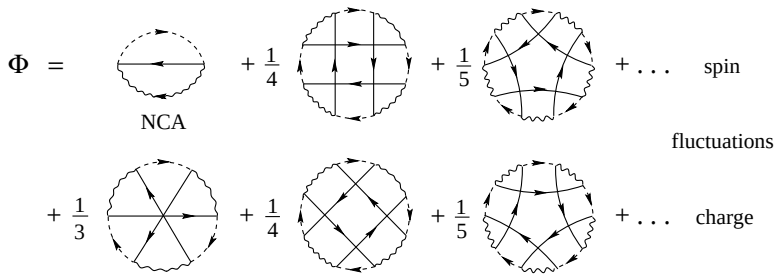

Fig. 3. Diagrammatic representation of the Luttinger-Ward functional generating the CTMA. The terms with the conduction electron lines running clockwise (labelled "spin fluctuations") generate $T^{(cf)}$, while the terms with the conduction electron lines running counter-clockwise (labelled "charge fluctuations") generate $T^{(cb)}$. The two-loop diagram is excluded, because it is not a skeleton.

The onset of a bound state is usually evidenced by a pole in the corresponding two–particle correlation function or T–matrix. Hence, one expects a pole in the singlet channel of the conduction electron–pseudofermion T–matrix $T^{(cf)}$. Taking a single slave boson propagator as the particle–particle (p–p) and particle–hole (p–h) irreducible $c-f$ vertex (leading order in V contribution), the equations for the $c-f$ p–h and p–p T–matrices are shown diagrammatically in Fig. 2 (1), (2). These contributions include, at any given order in the hybridization V, the maximum number of spin flips possible. Considering that in the mixed valence regime the Anderson model is dominated equally by spin and by charge fluctuations, one should also take the conduction electron–slave boson T–matrix $T^{(cb)}$ into account, which similarly includes the maximum number of charge fluctuation processes (see Fig. 2 (3)). The (linear) Bethe–Salpeter equations for $T^{(cf)}$, $T^{(cb)}$ read,

$$\begin{aligned} T^{(cf)}_{\sigma\tau,\sigma'\tau'}(i\omega_n, i\omega'_n, i\Omega_n) = \; & + \; V^2 G_b(i\omega_n + i\omega'_n - i\Omega_n)\delta_{\sigma\tau'}\delta_{\tau\sigma'} \\ & - \; V^2 T \sum_{\omega''_n} G_b(i\omega_n + i\omega''_n - i\Omega_n) \times \\ & G_{f\sigma}(i\omega''_n)\; G^0_c(i\Omega_n - i\omega''_n)\; T^{(cf)}_{\tau\sigma,\sigma'\tau'}(i\omega''_n, i\omega'_n, i\Omega_n) \end{aligned} \tag{12}$$

$$\begin{aligned} T^{(cb)\;\sigma}(i\omega_n, i\omega'_n, i\Omega_n) = & + \; V^2 G_{f\sigma}(+i\omega_n + i\omega'_n - i\Omega_n) \\ & - \; V^2 T \sum_{\omega''_n} G_{f\sigma}(i\omega_n + i\omega''_n - i\Omega_n) \times \\ & G_b(i\omega''_n)\; G^0_{c\sigma}(-i\omega''_n - i\Omega_n)\; T^{(cb)\;\sigma}(i\omega''_n, i\omega'_n, i\Omega_n). \end{aligned} \tag{13}$$

Inserting the NCA solutions for $G_{f\sigma}$, G_b into Eq. (12), one finds after an-

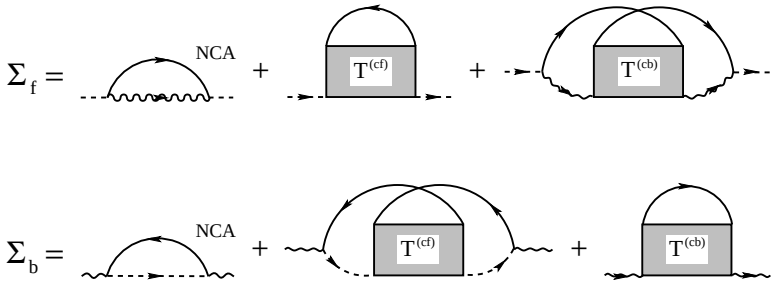

Fig. 4. Diagrammatic representation of the CTMA pseudofermion and slave boson self–energies Σ_f, Σ_b.

alytic continuation, as expected, a pole in the singlet channel of $T^{(cf)}$ at a center–of–mass frequency Ω_0 which scales with the Kondo temperature, $\Omega_0 \approx -T_K$. In order to incorporate this physics into the self–consistent scheme, we must construct a Luttinger–Ward functinal Φ which includes the total vertices $T^{(cf)}_{NCA}$, $T^{(cf)}$, $T^{(cb)}$ on the level of the self–energies. This functional is shown in Fig. 3 and consists of the sum of all slave particle rings where the bare hybridization vertices are connected by conduction electron lines in such a way that at most two other hybridization vertices are spanned. The set of self–energy terms deduced from Φ by functional differentiation is shown in Fig. 4. In the self–consistent scheme all propagators appearing in the self–energies are understood to be the fully renormalized ones. In order to avoid double counting of terms, the one-rung term in the second diagram of Σ_f and the one- and two-rung terms in the third diagram of Σ_f, Fig. 4 must be excluded. An analogous exclusion of terms must be done in Σ_b. For a detailed description see Ref. 21. Note that $T^{(cf)}_{NCA}$ just corresponds to a renormalization of the boson propagator by the NCA self–energy and, hence, is already included on the NCA level of self–consistent approximation. The self–consistent set of non–linear integral equations resulting from the definition of the self–energies Fig. 4 and the full Green's functions Eq. (6) is called CTMA. Solving the CTMA equations selfconsistently by iteration, the aforementioned pole is shifted to the threshold frequency $\Omega = 0$ where it merges with the continuous spectral density and thus renormalizes the threshold exponents. As signatures of the correct FL behavior below T_K it was found from the numerical solutions of the CTMA equations first that the correct FL exponents of the auxiliary particle propagators, Eq. (4), are reproduced within the error bars of the numerical solution, and second that the static impurity spin susceptibility χ shows Pauli behavior ($\chi(T) \approx const.$) for $T < T_K$ down to the lowest T considered, $T \approx 10^{-2} \cdot T_K$ (see Fig. 5).

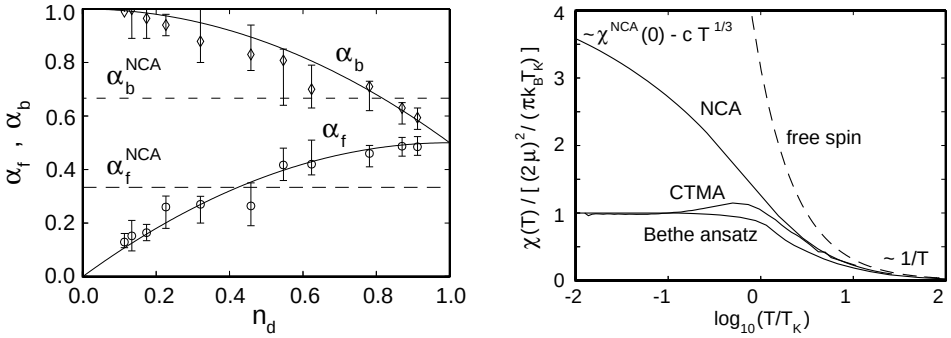

Fig. 5. Left panel: The fermion and boson threshold exponents α_f, α_b are shown for $N = 2$, $M = 1$ in dependence of the average impurity occupation n_d. Solid lines: exact values, Eq. (4); Symbols with error bars: CTMA; dashed lines: NCA. Right panel: Static susceptibility of the single-channel Anderson impurity model in the Kondo regime ($E_d = -0.8D$, $\Gamma = 0.1D$, Landé factor $g = 2$). The CTMA result is calculated using the The CTMA and NCA results are compared to the Bethe ansatz result for the Kondo model[38]. The CTMA susceptibility obeys scaling behavior in accordance with the exact results (not shown).

4. PERTURBATIVE RG ANALYSIS

Having introduced the CTMA as a method to describe quantum impurities in the strong coupling region, it is also important to know how it performs in the weak to intermediate coupling region, i.e. how within the CTMA the coupling constants for spin and potential scattering are renormalized in the sense of the perturbative renormalization group (RG). To obtain the correct weak to intermediate coupling renormalization within a self–consistent treatment turns out to be a non–trivial task. As seen below, not even within the NCA, which is a self–consistent expansion in the small parameter V (hybridization), the correct weak coupling renormalization is produced for the Anderson impurity model.

In this section the coupling constant renormalization for spin and potential scattering will be analyzed within the perturbative RG[41,42]. In doing so we will assume to be in the Kondo regime of the Anderson model, where $E_d < 0$ and $\Gamma/|E_d| \ll 1$.

In the (anisotropic) Kondo model the local spin–conduction electron interaction vertex is defined as

$$J_\perp(S^+\sigma^- + S^-\sigma^+) + J_{||}S_z\sigma_z \ . \tag{14}$$

For isotropic coupling, $J_\perp = J_{||} = J$, this reduces to the regular Heisenberg

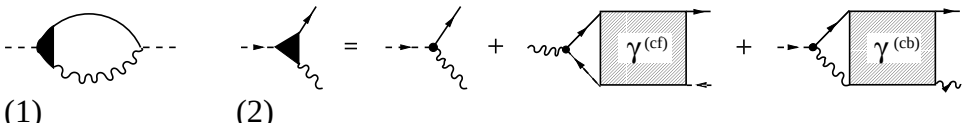

Fig. 6. (1) The fermion selfenergy expressed in terms of the exact 3–point vertex $\hat{V}$ (black triangle) is shown. (2) Representation of $\hat{V}$ in terms of the 4–point vertices γ^{cf}, γ^{cb}. The first diagram on the right–hand side is the bare 3–point vertex V.

coupling $J\,\vec{S}\cdot\vec{\sigma}$. In the above expressions $\vec{S} = (S_x, S_y, S_z)$ denotes the impurity spin 1/2 vector operator and $\vec{\sigma} = (\sigma_x, \sigma_y, \sigma_z)$ the vector of Pauli matrices. $S^{\pm}$ and $\sigma^{\pm}$ are the spin raising (+) and lowering (-) operators for the local and for the conduction electron spin, respectively. In addition, there may be a potential scattering term which has the structure

$$W\,(\mathbf{1}\,\mathbf{1}) \tag{15}$$

with $\mathbf{1}$ the 2×2 unit matrix in impurity and in conduction electron spin space.

Since in the Anderson model the hybridization V (Eq. (1)) appears as the bare coupling constant, but not the spin and potential scattering couplings $J_\perp$, $J_{||}$, and W, the NCA or CTMA self–energies must first be represented in terms of the 4–point spin and potential vertices. This is done as follows for the pseudofermion self–energy Σ_f. We note that it is not necessary to consider separately the boson self–energy Σ_b here, since Σ_b will appear naturally as a coupling constant renormalization in the perturbative RG. The (exact) Σ_f can be written in terms of the exact, total 3–point hybridization vertex $\hat{V}$ in slave boson representation as (see Fig. 6 (1))

$$\begin{aligned}\Sigma_{f\sigma}(\omega - i0) \;&=\; V\int\frac{d\varepsilon}{2\pi}f(\varepsilon)G_b^0(\varepsilon+\omega-i0)\times \\ &\left[\hat{V}(\omega-i0,\varepsilon+i0)\,G_{c\sigma}^0(-\varepsilon-i0) - \hat{V}(\omega-i0,\varepsilon-i0)\,G_{c\sigma}^0(-\varepsilon+i0)\right],\end{aligned} \tag{16}$$

where G_b^0 is the bare boson Green's function, Eq. (8). The total 3–point vertex $\hat{V}$ can in turn be expressed in terms of the exact, total 4–point c–f and c–b vertices γ^{cf}, γ^{cb}, as shown in Fig. 6 (2). These 4–point vertices are comprised of all vertex corrections connecting the f and the c line or the b and the c line of the 3–point vertex $\hat{V}$, respectively. Note that vertex corrections connecting the f and b lines do not appear as these are of higher order in the fugacity $\mathrm{e}^{-\beta\lambda}$ and thus vanish under projection onto the physical subspace. A given approximation for the selfenergy Σ_f (like NCA or CTMA) corresponds to a respective approximation for γ^{cf}, γ^{cb}.

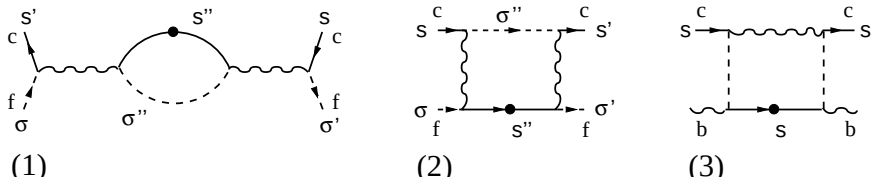

Fig. 7. perturbative RG renormalizations of the (irreducible) c–f vertex. Diagram (1) is the NCA result, the sum of diagrams (1), (2) the result of CTMA. (3) ist the contribution from the c–b vertex, which is not scaling. The black dots on the conduction electron lines indicate that the frequency integrals in those lines are restricted to the region $[-D, -D + dD]$.

The perturbative RG analysis can now be applied to the Bethe–Salpeter equations for the total vertices (T–matrices) γ^{cf}, γ^{cb}, thus determining the RG flow of the spin and potential scattering coupling constants within the given approximation. Note that for the *perturbative* RG treatment all propagator lines appearing are the bare ones, while in the self–consistent treatment described above all propagators are fully renormalized.

4.1. Perturbative RG for the NCA

Inserting the "RPA–like" T–matrix $T^{(cf)}_{NCA}$ for γ^{cf} and the resulting $\hat{V}$ into Eq. (16) for the f self–energy, it is seen that the NCA is just defined by

$$\gamma^{cf} = T^{(cf)}_{NCA} \tag{17}$$

$$\gamma^{cb} = 0 \ , \tag{18}$$

and $T^{(cf)}_{NCA}$ provides just the renormalization of the boson propagator by the NCA self–energy, as mentiond above. Integrating out the high energy region from the Bethe–Salpeter equation for $T^{(cf)}_{NCA}$ and applying the usual perturbative poor man's scaling analysis[41,42], we obtain for the renormalization of the irreducible conduction electron–pseudofermion vertex under a change of the high energy cutoff from D to $D - dD$ (compare Fig. 7 (1))

$$d\Lambda^{(cf)} = -N_0 \frac{dD}{D} \sum_{s''\sigma''} [\Lambda^{(cf)}]_{s'\sigma'',s''\sigma} [\Lambda^{(cf)}]_{s''\sigma',s\sigma''} \tag{19}$$

where the spin indices s, s', s'', σ, σ', σ'', are as defined in Fig. 7 (1) and the (unrenormalized) c–f vertex is given by the inhomogeneous part of the Bethe–Salpeter equation (12) [see also Fig. 2 (2)],

$$\Lambda^{(cf)}_{s'\sigma',s\sigma} = [J_\perp (S^+\sigma^- + S^-\sigma^+) + J_{||} S_z \sigma_z + W\mathbf{1}]_{s'\sigma',s\sigma} \ . \tag{20}$$

In Eq. (20) s, s' denote the conduction electron spin indices, σ, σ' the impurity spin indices, where an index with (without) prime represents an ingoing (outgoing) particle. For the Anderson model we have $J_\perp = J_{||} = 2W = V^2/|E_d|$, the $|E_d|^{-1}$ arising from the bare boson propagator, Eq. 8, taken at frequencies $|\omega| \ll |E_d|$. However, for generality we keep the anisotropic couplings $J_\perp$, $J_{||}$, W in the above equations. $d\Lambda^{(cf)}$ may be simplified as

$$\begin{aligned} d\Lambda^{(cf)} = -N_0 d\ln D \quad & \Big[\quad (J_{||}J_\perp + 2WJ_\perp)[S^+\sigma^- + S^-\sigma^+] \\ & + \quad (J_\perp^2 + 2WJ_{||})[S_z\sigma_z] \\ & + \quad (\frac{1}{2}J_\perp^2 + \frac{1}{4}J_{||}^2 + W^2)[\mathbf{11}]\Big] \ . \end{aligned} \tag{21}$$

Hence, within NCA we have the RG equations

$$\frac{dJ_\perp}{d\ln D} = -N_0(J_{||}J_\perp + 2WJ_\perp) \tag{22}$$

$$\frac{dJ_{||}}{d\ln D} = -N_0(J_\perp^2 + 2WJ_{||}) \tag{23}$$

$$\frac{dW}{d\ln D} = -N_0(\frac{1}{2}J_\perp^2 + \frac{1}{4}J_{||}^2 + W^2) \ . \tag{24}$$

For the initial conditions of the Anderson impurity case, $J_{\perp,0} = J_{||,0} = 2W_0 = V^2/|E_d| = J_0$, these are easily integrated to give

$$J(D) = \frac{J_0}{1 + 2N_0 J_0 \ln\frac{D}{D_0}} \ , \tag{25}$$

i.e. the spin coupling constant diverges at the Kondo temperature $T_K = D_0 \mathrm{e}^{-1/(2N_0J_0)}$. However, the potential scattering coupling is also renormalized under the RG flow. Thus, within NCA there is a spurious divergence of the potential scattering term at T_K as well. The fact that within NCA potential scattering is incorrectly treated on the same footing as spin scattering may be traced back to be the origin why (1) within NCA the asymmetry of the Kondo resonance comes out too large and why (2) NCA gives a qualitatively wrong descripting of the Kondo resonance in a magnetic field [39].

4.2. Perturbative RG for the CTMA

We now consider the coupling constant renormalization under the RG flow within CTMA. The CTMA f self–energy (Fig. 4) is generated by inserting, in addition to the NCA contribution, the ladder T–matrices, Eqs. (12),

(13), for $\gamma^{(cf)}$, $\gamma^{(cb)}$. This is seen by comparing Fig. 6 with Fig. 4.[40] i.e. we have *in addition* to the vertices of the previous section,

$$\gamma^{cf} = T^{(cf)} \tag{26}$$
$$\gamma^{cb} = T^{(cb)} \ . \tag{27}$$

The resulting *additional* c–f vertex renormalization under cutoff reduction is (see Fig. 7 (2))

$$d\Lambda^{(cf)} = +N_0 \frac{dD}{D} \sum_{s''\sigma''} [\Lambda^{(cf)}]_{s'\sigma',s''\sigma''} [\Lambda^{(cf)}]_{s''\sigma'',s\sigma} \ , \tag{28}$$

which can again be simplified as

$$\begin{aligned} d\Lambda^{(cf)} = +N_0 d\ln D \quad \Big[& \quad (-J_{||}J_\perp + 2WJ_\perp)[S^+\sigma^- + S^-\sigma^+] \\ + & \quad (-J_\perp^2 + 2WJ_{||})[S_z\sigma_z] \\ + & \quad (\frac{1}{2}J_\perp^2 + \frac{1}{4}J_{||}^2 + W^2)[\mathbf{11}]\Big] \ . \end{aligned} \tag{29}$$

Finally, we also need to investigate the renormalization due to $\gamma^{(cb)}$ (Fig. 7 (3)). This term is obviously diagonal in spin space (potential scattering). Its amplitude is

$$\begin{aligned} d\Lambda^{(cb)} &= -N_0 V^4 \int_{-D}^{-D+dD} d\varepsilon \times \\ & \qquad G^0_{f\sigma}(\omega+\varepsilon) G^0_{f\sigma}(\omega'+\varepsilon) G^0_b(\varepsilon-\Omega)\Big|_{\Omega=0,\omega,\omega',\varepsilon \ll D < |E_d|} \\ &= -N_0 \frac{V^4}{|E_d|}\frac{dD}{D^2} \ , \end{aligned} \tag{30}$$

or, with $W = V^2/(2|E_d|)$,

$$dW = -4N_0|E_d|W^2\frac{dD}{D^2} \ . \tag{31}$$

This correction is not logarithmic (non-scaling), and the integration of Eq. (31) yields a nondivergent result. Hence, it need not be considered in the RG flow.

Adding up the contributions Eqs. (21) and (29) it is seen that the potential terms always cancel each other. Thus, there is no renormalization of the potential term. The resulting RG equations of the CTMA are

$$\frac{dJ_\perp}{d\ln D} = -2N_0 J_{||} J_\perp \tag{32}$$

$$\frac{dJ_{||}}{d\ln D} = -2N_0 J_\perp^2 \tag{33}$$

$$\frac{dW}{d\ln D} = 0\ . \tag{34}$$

These are identical to the perturbative RG equations of the original Kondo model. This proves that the CTMA incorporates the complete Kondo physics also in the weak and intermediate coupling regime, where the perturbative RG is valid.

5. CONCLUSION

We have given an overview of a diagrammatic, conserving approximation the CTMA, designed to describe quantum impurity systems of the Anderson type in the strong coupling regime. By means of a perturbative renormalization group analysis it was shown that, in contrast to an earlier approximation (NCA) it recovers the correct RG flow in the weak to intermediate coupling region. In particular, it describes correctly, that potential scattering terms do not scale in the Kondo and Anderson problems, while the correct Kondo scale for the divergence of the spin dependent part is recovered. Together with the fact that in numerical solutions of the CTMA the auxiliary particle threshold exponents and the spin susceptibility show the correct Fermi liquid behavior of the strong coupling regime, this provides evidence that the CTMA correctly describes the Anderson model both in the strong and in the weak coupling regime on the same footing. It has also the potential to be generalized to describe more complicated situations and lattice problems by use of the DMFT.

ACKNOWLEDGMENTS

It is our pleasure to thank Peter Wölfle who has provided continuing support and guidance throughout the progress of the CTMA project. We would also like to thank A. Rosch, G. Sellier, P. Hirschfeld, T. Kopp, K. Haule and T. Schauerte for valuable discussions. This work was supported by DFG through SFB195.

REFERENCES

1. For a comprehensive overview see A. C. Hewson, *The Kondo Problem to Heavy Fermions* (C.U.P., Cambridge, 1993).
2. W. Metzner and D. Vollhardt, *Phys. Rev. Lett.* **62**, 324 (1989).
3. A. Georges, G. Kotliar, W. Krauth, and M. J. Rozenberg, *Rev. Mod. Phys.* **68**, 13 (1996).
4. L. I. Glazman, and M. E. Raikh, *Pis'ma Zh. Eksp. Teor. Fiz.* **47**, 378 (1999) [*JETP Lett.* **47**, 452 (1988)].
5. T. K. Ng, and P. A. Lee, *Phys. Rev. Lett.* **61**, 1768 (1988).
6. For an overview and references see, e.g., *Quantum dynamics of submicron structures*, H. A. Cerdeira, B. Kramer, and G. Schön, eds., NATO ASI Series E **291** (Kluwer, 1995).
7. J. Li, W.-D. Schneider, R. Berndt, and B. Delley, *Phys. Rev. Lett.* **80**, 2893 (1998).
8. V. Madhavan, W. Chen, T. Jamneala, M. F. Crommie, and N. S. Wingreen, *Science* **280**, 567 (1998).
9. O. Újsǵhy, J. Kroha, L. Szunyogh, and A. Zawadowski, *Phys. Rev. Lett.* **85**, 2557 (2000).
10. M. Garnier, K. Breuer, D. Purdie, M. Hengsberger, Y. Baer, and B. Delley, *Phys. Rev. Lett.* **78**, 4127 (1997).
11. F. Reinert, D. Ehm, S. Schmidt, G. Nicolay, S. Hüfner, J. Kroha, O. Trovarelli, and C. Geibel, *Phys. Rev. Lett.* **87**, 106401 (2001).
12. S. E. Barnes, *J. Phys. F* **6**, 1375 (1976); **7**, 2637 (1977).
13. D. Goldhaber–Gordon *et al.*, *Nature* **391**, 156 (1998).
14. S. M. Cronenwett, T. H. Osterkamp, and L. P. Kouwenhoven, *Science* **281**, 540 (1998).
15. J. Schmid, J. Weis, K. Eberl, and K. v. Klitzing, *Physica B* **258**, 182 (1998).
16. J. Kroha, P. Hirschfeld, K. A. Muttalib, and P. Wölfle, *Solid State Comm.* **83** (12), 1003 (1992).
17. J. Kroha, P. Wölfle, and T. A. Costi, *Phys. Rev. Lett.* **79**, 261 (1997).
18. T. Schauerte, J. Kroha, and P. Wölfle, *Phys. Rev. B* **62**, 4394 (2000).
19. K. Haule, S. Kirchner, J. Kroha, and P. Wölfle, *Phys. Rev. B* **64**, 155111 (2001).
20. J. Kroha and P. Wölfle, *Festkrperprobleme/Adv. Solid State Phys.* **39**, 271 (1999).
21. J. Kroha and P. Wölfle, in *Proceedings of the International Conference on "Mathematical Methods in Physics"*, Montreal 2000, D. Senechal, ed., in press (Springer, 2001); cond-mat/0105491.
22. J. Kroha and P. Wölfle, *Acta Phys. Pol. B* **29**, 3781 (1998); cond-mat/9811074.
23. A. Rosch, private communication.
24. A. A. Abrikosov, *Physics* **2**, 21 (1965).
25. P. Coleman, *Phys. Rev. B* **29**, 3035 (1984).
26. G. Baym and L.P. Kadanoff, *Phys. Rev.* **124**, 287 (1961); G. Baym, *Phys. Rev.* **127** 1391 (1962).
27. P. Nozières and C. T. De Dominicis, *Phys. Rev.* **178**, 1073; 1084; 1097 (1969).
28. P. W. Anderson, *Phys. Rev. Lett.* **18**, 1049 (1967).
29. B. Menge and E. Müller-Hartmann, *Z. Phys. B* **73**, 225 (1988).

30. K. D. Schotte and U. Schotte, *Phys. Rev.* **185**, 509 (1969).
31. T. A. Costi, P. Schmitteckert, J. Kroha, and P. Wölfle, *Phys. Rev. Lett.* **73**, 1275 (1994); *Physica* (Amsterdam) **235-240C**, 2287 (1994).
32. S. Fujimoto, N. Kawakami and S. K. Yang, *J. Phys. Korea* **29**, S136 (1996).
33. I. Affleck and A. W. W. Ludwig, *Nucl. Phys. B* **352**, 849 (1991); **360**, 641 (1991); *Phys. Rev. B* **48**, 7297 (1993).
34. T.A. Costi, J. Kroha, and P. Wölfle, *Phys. Rev. B* **53**, 1850 (1996).
35. H. Keiter and J. C. Kimball, *J. Appl. Phys.* **42**, 1460 (1971); N. Grewe and H. Keiter, *Phys. Rev. B* **24**, 4420 (1981).
    4420 (1981).
36. Y. Kuramoto, *Z. Phys. B* **53**, 37 (1983); H. Kojima, Y. Kuramoto and M. Tachiki, *ibid.* **54**, 293 (1984); Y. Kuramoto and H. Kojima, *ibid.* **57**, 95 (1984); Y. Kuramoto, *ibid.* **65**, 29 (1986).
37. E. Müller–Hartmann, *Z. Phys. B* **57**, 281 (1984).
38. N. Andrei, K. Furuya, J. H. Löwenstein, *Rev. Mod. Phys.* **55**, 331 (1983).
39. G. Sellier, J. Kroha, and P. Wölfle, in preparation.
40. Note that the single–rung term of $T^{(cf)}$ or $T^{(cb)}$, when inserted for $\gamma^{(cf)}$ or $\gamma^{(cb)}$, respectively, into the 3–point verex $\hat{V}$, does not lead to an allowed diagram. However, the corresponding self–energy terms containing two (bare) boson (fermion) lines are already included in the NCA (see section 4.1). Also note that in order to avoid double counting, the two-rung terms have to be subtracted from $T^{(cf)}$ or $T^{(cb)}$. Since these are, however, a finite number of terms, they do not contribute to the re-scaling and can be neglected in the RG analysis.
41. P. W. Anderson and G. Yuval, *Phys. Rev. Lett.* **23**, 89 (1969).
42. P. W. Anderson, *J. Phys. C* **3**, 2439 (1970).